Journal of Advances in Science and Technology
Vol. 13, Issue No. 2, March-2017, ISSN 2230-9659

Study on Nuclear Structure and Decay

Nidhi Sharma*

M.Sc. Physics, B.Ed., #449, Sector-13, Urban Estate, Kurukshetra, Haryana, India

Abstract – The study of nuclear properties shows evidence of nuclear shells analogous to those observed in the atoms. One clear piece of evidence in the nuclear case is the sharp discontinuity in nucleon separation energies for certain numbers of N and Z known as magic numbers. In the case of the electronic shells in atoms the picture is very clear, since there is a central Coulomb potential, due to the charge carried by the nucleus and electrons. In the case of the nucleus there is no such external potential but the nucleons move in the potential created by themselves. This potential contains many terms: central, spin-orbit, tensor, spin spin, etcFor nuclei farther from the magic numbers one must add the assumption that due to the relation between the strong nuclear force and angular momentum, protons or neutrons with the same ntend to form pairs of opposite angular momenta. Therefore a nucleus with an even number of protons and an even number of neutrons has 0 spin and positive parity. A nucleus with an even number of protons and an odd number of neutrons (or vice versa) has the parity of the last neutron (or proton), and the spin equal to the total angular momentum of this neutron (or proton).

Key Words:- nuclear Structure, Electromagnetic Decays, Nilsson Term, Magic Numbers

--------------------------♦-----------------------------

INTRODUCTION

Igal Talmi developed a method to obtain the information from experimental data and use it to calculate and predict energies which have not been measured. This method has been successfully used by many nuclear physicists and has led to deeper understanding of nuclear structure. The theory which gives a good description of these properties was developed. This description turned out to furnish the shell model basis of the elegant and successful Interacting boson model. We can imagine ourselves building a nucleus by adding protons and neutrons. These will always fill the lowest available level. Thus the first two protons fill level zero, the next six protons fill level one, and so on. As with electrons in the periodic table, protons in the outermost shell will be relatively loosely bound to the nucleus if there are only few protons in that shell, because they are farthest from the center of the nucleus. Therefore nuclei which have a full outer proton shell will have a higher binding energy than other nuclei with a similar total number of protons. All this is true for neutrons as well. This means that the magic numbers are expected to be those in which all occupied shells are full. We see that for the first two numbers we get 2 (level 0 full) and 8 (levels 0 and 1 full), in accord with experiment. However the full set of magic numbers does not turn out correctly. Low-lying energy levels in a single-particle shell model with an oscillator potential (with a small negative l2 term) without spin-orbit (left) and with spin-orbit (right) interaction. The number to the right of a level indicates its degeneracy, (2j+1). The boxed integers indicate the magic numbers. Together with the spin-orbit interaction, and for appropriate magnitudes of both effects, one is led to the following qualitative picture: At all levels, the highest j states have their energies shifted downwards, especially for high n (where the highest j is high). This is both due to the negative spin-orbit interaction energy and to the reduction in energy resulting from deforming the potential to a more realistic one. The second-to-highest j states, on the contrary, have their energy shifted up by the first effect and down by the second effect, leading to a small overall shift. The shifts in the energy of the highest j states can thus bring the energy of states of one level to be closer to the energy of states of a lower level. The "shells" of the shell model are then no longer identical to the levels denoted by n, and the magic numbers are changed.

EXPERIMENTAL

Low-lying energy levels in a single-particle shell model with an oscillator potential (with a small negative l^2 term) without spin-orbit (left) and with spin-orbit (right) interaction. The number to the right of a level indicates its degeneracy, ($2j+1$). The boxed integers indicate the magic numbers. We may then suppose that the highest j states for n = 3 have an intermediate energy between the average energies of n = 2 and n = 3, and suppose that the highest j states for larger n (at least up to n = 7) have an energy closer to the average energy of $n-1$. Then we get the following shells (see the figure)

- 1st shell: 2 states (n = 0, j = ½).

- 2nd shell: 6 states (n = 1, j = $^1/_2$ or $^3/_2$).
- 3rd shell: 12 states (n = 2, j = $^1/_2$, $^3/_2$ or $^5/_2$).
- 4th shell: 8 states (n = 3, j = $^7/_2$).
- 5th shell: 22 states (n = 3, j = $^1/_2$, $^3/_2$ or $^5/_2$; n = 4, j = $^9/_2$).
- 6th shell: 32 states (n = 4, j = $^1/_2$, $^3/_2$, $^5/_2$ or $^7/_2$; n = 5, j = $^{11}/_2$).
- 7th shell: 44 states (n = 5, j = $^1/_2$, $^3/_2$, $^5/_2$, $^7/_2$ or $^9/_2$; n = 6, j = $^{13}/_2$).
- 8th shell: 58 states (n = 6, j = $^1/_2$, $^3/_2$, $^5/_2$, $^7/_2$, $^9/_2$ or $^{11}/_2$; n = 7, j = $^{15}/_2$).

and so on.

The magic numbers are then

- 2
- 8=2+6
- 20=2+6+12
- 28=2+6+12+8
- 50=2+6+12+8+22
- 82=2+6+12+8+22+32
- 126=2+6+12+8+22+32+44
- 184=2+6+12+8+22+32+44+58

and so on. This gives all the observed magic numbers, and also predicts a new one (the so-called island of stability) at the value of 184 (for protons, the magic number 126 has not been observed yet, and more complicated theoretical considerations predict the magic number to be 114 instead).

Another way to predict magic (and semi-magic) numbers is by laying out the idealized filling order (with spin-orbit splitting but energy levels not overlapping). For consistency s is split into j = 1⁄2 and j = -1⁄2 components with 2 and 0 members respectively. Taking leftmost and rightmost total counts within sequences marked bounded by / here gives the magic and semi-magic numbers.

- s(2,0)/p(4,2)> 2,2/6,8, so (semi)magic numbers 2,2/6,8
- d(6,4):s(2,0)/f(8,6):p(4,2)> 14,18:20,20/28,34:38,40, so 14,20/28,40
- g(10,8):d(6,4):s(2,0)/h(12,10):f(8,6):p(4,2)>

  50,58,64,68,70,70/82,92,100,106,110,112, so 50,70/82,112
- i(14,12):g(10,8):d(6,4):s(2,0)/j (16,14):h(12,10):f(8,6):p(4,2)> 126,138,148,156,162,166,168,168/184,198,210,220,228,234,238,240, so 126,168/184,240

Note that the rightmost predicted magic numbers of each pair within the quartets bisected by / are double tetrahedral numbers from the Pascal Triangle: 2,8,20,40,70,112,168,240 are 2x 1,4,10,20,35,56,84,120..., and the leftmost members of the pairs differ from the rightmost by double triangular numbers: 2-2=0, 8-6=2, 20-14=6, 40-28=12, 70-50=20, 112-82=30, 168-126=42, 240-184=56, where 0,2,6,12,20,30,42,56... are 2x 0,1,3,6,10,15,21,28....

ANALYSIS OF NUCLEAR STRUCTURE & DECAY

To check the level of reliability for the angular distribution analysis in the current work, tests were made with transitions of known multi polarity. The results from two known prompt transitions are shown in Fig. for ^{198}Pt ($4^+ \rightarrow 2^+$) 578 keV, E2 transition and ^{138}Ba ($9^- \rightarrow 8^+$) 449 keV, E1 transition. The angular distribution coefficients A^2 were deduced to be A^2 = 0.21±0.18 and A2 = −0.18±0.14 respectively for these transitions. These angular distributions are consistent with previous findings, supporting the current analysis, at least at the 1σ level. The fitted curves for the prompt γ rays above the proposed 10^+ isomer in ^{136}Ba are shown in Fig. The angular distribution coefficients A_2 the A_4 coefficient is neglected in the fit found from fitting the slope of the intensities as a function of $\cos^2 \theta$ are listed in Table . The spin and parity assignments for the states identified above the isomer are somewhat problematic due to the significant uncertainties in the measured angular distributions. These result in making most values consistent with no measurable anisotropy at the 2σ level. However, the data suggests that the 349 keV is consistent with a dipole decay at the 1σ level. The nucleus ^{136}Ba has six valence protons outside the closed shell at Z = 50 and 2 neutron holes with respect to the closed shell at N = 82. It was pointed out in 1973 by Meyer-Levy and Lopac that many of the low-lying properties of the N = 80 isotones might be explained by the simple coupling of the two-neutron holes to a quadrupole vibrator core. The authors of Ref. also noted that the spectral pattern of the N = 80 isotones from ^{132} Te up to ^{140} Nd were rather similar with the presence of a two-phonon, quadrupole vibrational triplet established for ^{136}Ba and its neighbour, ^{138}Ce. This work ignored any effects from the proton particles and allowed couplings of neutron-hole states from the $d^{3/2}$, $s^{1/2}$, $h^{11/2}$, $d^{5/2}$ and $g^{7/2}$ orbitals to a vibrational core. While this approach gave a reasonable prediction for the energies of the low-lying negative-parity states and the first 2^+ and 4^+ levels, it predicted that the yrast 6^+ and 8^+ states lay above the yrast 10^+ level. This clearly pointed to the need to include proton and neutron degrees of freedom in the calculations for such apparently simple, two-neutron whole systems.

RESULTS AND DISCUSSION

A large number of isomeric states populated in the reaction have been identified in the beam and target-like regions. Figure shows the different isomers populated that range from ^{50}Sn to ^{140}Ce for BLFs while for TLFs the isomers range from ^{180}Ta to ^{206} Po. This figure also shows the N/Z equilibration line for the BLFs and TLFs. The majority of nuclei populated in the reaction lie above the N/Z equilibration line, while not many nuclei have been populated below the N/Z equilibration line. A number of previously unreported isomers populated in the target-like region have been observed in ^{201}Tl, ^{195}Au, ^{198}Pt, ^{194}Os, ^{192}Os, ^{191}Os and ^{184}W, while new isomers populated in the beam-like region include those in ^{139}La, ^{136}Ba, ^{131}I, ^{133}I and ^{127}Sb. The following sections will concentrate mainly on the structure of ^{136} Ba, ^{184} W, ^{198}Pt and ^{194}Os. Figures show the background subtracted γ-ray spectra for some selected isomers populated in the beam-like and target-like regions respectively. Also shown are the fitted half-life curves for those decays. Figures show the background subtracted γ-ray spectra for some isomers in the beam-like and target like regions whose exact half-lives could not be determined but it was possible to put a limit to their half-lives. The experimental set-up used was sensitive to half-lives. Nuclei in the vicinity of the doubly-closed-shell nucleus ^{132} Sn_{82} give information on the basic single particle structure and interactions between pairs of nucleons occupying the valence states. In particular, the evolution of structure in the N = 80 isotones can be used to identify the pertinent role of the unnatural-parity h11/ 2 neutron orbital which has a major influence on the make-up of the high-spin states in this region. Isomeric I = 10^+ states have been reported in all the even-A, N = 80 isotones from ^{130} Sn up to ^{148} Er with the exception of the Z = 56 isotone, ^{136}Ba. In the recent paper by Genevey ,the significant reduction of the B(E2) between the yrast 10^+ isomeric state and the first 8+ state in the Z ≥ 58, N = 80 isotones compared to their Z ≤ 54 counterparts has been discussed in terms of a significant component

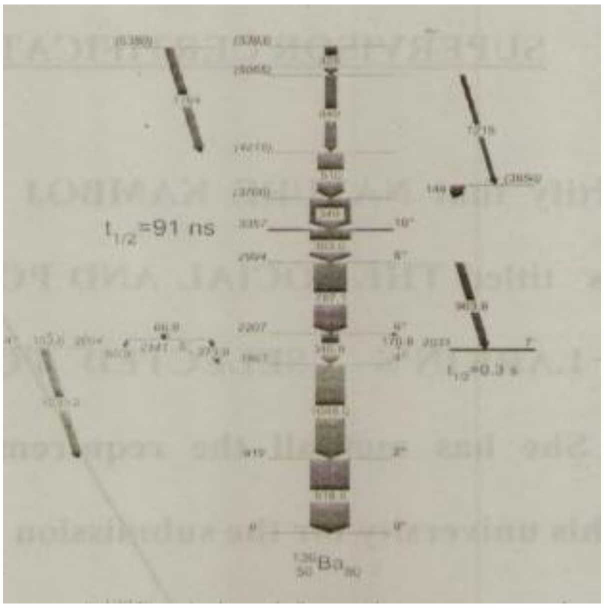

Figure : Level scheme of 136Ba deduced from the present work with the 91 +2 ns I_ = 10+ isomer. The widths of the arrows are proportional to the relative γ-ray intensities. Note that all the energies are given in keV. of the neutron configuration in the wavefunction of the state in the lighter systems. The magnetic moment measurements of the yrast I = 10^+ isomers in ^{138} Ce and ^{140} Nd are all consistent with near-spherical, maximally-aligned two neutronhole, configurations. Similar, two-neutron-hole I = 10^+ states have also been observed in the lighter barium isotopes, ^{132} Ba and ^{134} Ba. Prior to this study, the medium-to-high-spin data on ^{136}Ba were restricted due to the β-stable nature of ^{136}Ba, which makes it difficult to populate with heavy-ion induced fusion-evaporation reactions. The N = 80 isotone lies between the lighter barium isotopes which can be readily populated using this method and heavier, neutron-rich isotopes which have been studied as residues from spontaneous fission . To date, the data on the near-yrast states in ^{136}Ba comes from work using β decay (n, γ) reactions Coulomb excitation and light-ion induced fusion reactions As a result, prior to this work, the highest spin state known was the yrast 8^+ state identified by Dragulescu. The level scheme deduced from the present work for ^{136}Ba is shown in Fig. and was obtained by examining background subtracted spectra from: i) an out-of-beam matrix, constructed from delayed γ − γ coincidences for the levels below the the 10^+ isomer. ii) an in-beam prompt matrix, constructed from γ−γ coincidences gated on delayed transitions in ^{136}Ba and Doppler corrected for the BLFs . This enabled the identification of prompt transitions which feed the 10^+ isomer. iii) a prompt-delayed matrix which corresponded to pairs of γ rays in which the first one came as a prompt, in-flight decay, while the delayed transition was measured between 45 and 780 ns later.

The observation of the 819 keV ($2^+ \rightarrow 0^+$) transition in ^{136}Ba in the delayed spectrum shown in Fig. demonstrates the presence of an isomer in this nucleus. Figure shows all the transitions up to the previously reported 8^+ state, together with a transition at 363 keV, which is interpreted to be the direct decay from a 10^+ isomer. The excitation energy of this isomer is established from the γ−γ coincidence relationships to be 3357 keV. Spins and parities have been established for the levels in 136Ba up to the $I = 8^+$ state at 2994 keV . The $I = 8^+$ state at 2994 keV which decays to the $I = 6^+$ state via a γ ray of energy 787 keV, is observed in the present work together with a previously unreported branch which decays to the I = 7 isomeric state at 2031 keV via a 964 keV transition. The multipolarity of the 363 keV transition could be E1, E2 or M1, from the intensity balance across the 2994 keV state.

CONCLUSION

The measurement of the angular distribution of a γ-ray transition can help to determine the multi polarity of the transition and consequently the spins of the excited nuclear states. The nuclei produced in a fusion-evaporation reaction, for example, are aligned with the angular momentum vector perpendicular to the beam direction. It is therefore possible to obtain an anisotropic angular distribution. If there is no prefered direction, the angular distributions are isotropic. The initial alignment of the nucleus can be smeared out by the emission of evaporated particles. The angular distribution formula is given by

$$\mathbf{W(\theta) = \sum Ak\ Pk(\cos\theta)}$$

where W(θ) is the γ-ray intensity measured at angle θ to the beam direction. In the case of γ-ray emissions, where the parity is conserved, only k=even numbers are considered, less than or equal to 2I where I is the angular momentum taken away by the emitted photon. Pk(cos θ) are the standard Legendre polynomials and the Ak are the angular distribution coefficients. The Ak value depends on the m-population distribution and the I_{Π} values of the initial and final states. For an electric dipole transition ∆L = 1, or magnetic dipole transition , W(θ) will be given by

$$\mathbf{W(\theta) = A_0(1 + A_2P_2(\cos\theta))}$$

where $P_2(\cos\theta) = 1/\ 2\ (\cos 2\theta - 1)$ and A0 is the “true” intensity. For an electric quadrupole (E2) transition ∆L = 2, or magnetic quadrupole transition (M2), the angular distribution will be given by

$$\mathbf{W(\theta) = A_0(1 + A_2P_2(\cos\theta) + A_4P_4(\cos\theta))}$$

where $P_4 = 1/\ 8\ (35 \cos^4\theta - 30 \cos^2\theta + 3)$.

Experimentally, the dependence of the γ-ray intensity versus the polar angle of the γ detectors will be directly measured. In this thesis those angles will be given by the germanium detectors of Gammasphere.

The Chico detector consists of 20 separate trapezoidal Parallel Plate Avalanche Counters. The essential elements of each PPAC comprise a thin film anode, segmented in two unequal parts, plus a cathode circuit board which is segmented into 1◦ wide traces of constant polar angle θ. There are two identical hemispherical assemblies, each of which houses 10 of the PPACs arranged in a truncated cone coaxial with the beam direction. Figure shows one hemisphere of the Chico detector installed in one half of Gamma sphere. The forward assembly, note that the backward one was not used during the experiment described in this thesis, due to the forward focused reaction kinematics, has an active θ range from 12◦ to 85◦. An individual PPAC covers an azimuthal width of 28◦ and there is a dead region of 8◦ in φ between each of the PPACs. For the set-up including both hemispheres, this provides 280◦ of φ coverage for both the forward and backward assemblies. The total angular coverage is approximately 2.8π sr, corresponding to about 69% of the total solid angle. Chico has been designed to measure the azimuthal φ and the polar θ angles with respect to the beam direction of the scattered nuclei, and the Time-Of-Flight difference. The azimuthal angle φ is measured using the segmentation of the anodes. To measure φ a “binary” scheme was implemented. The anodes are segmented into two sections covering 1/3 and 2/3 of the total φ angle subtended by the individual PPACs. Chico is used mostly for binary reactions, therefore two-body kinematics demands that the scattered target and beam-like fragments are coplanar to first order note that the emission of light particles, such as neutrons, will shift the fragments slightly out of plane. As a result of using a thin target, the beam and target-like reaction fragments, BLFs and TLFs respectively, produced in the binary reaction, could be detected using Chico in coincidence with the γ rays emitted by the nuclei of interest. The ∆TOF measured between the detection of the two fragments and the angular information directly given by the recoil detector allows the separation of the BLFs and TLFs. Figure shows the separation between the two binary partners, with the most intense peak lying in the vicinity of the grazing angle which for this particular reaction occurs at the same laboratory angle, 50◦, for both the TLFs and BLFs. Figure shows the angular correlation of the two coplanar scattered nuclei detected in two opposing PPACs. Figures show a cut-off at 20◦ as a result of the use of a mask to stop the high counting rate at low angles. The reduction in counts in these spectra at 60◦ occurs as a result of a support rib in the pressure window of Chico and could be used for internal angular calibration purposes. Figure shows that at low angles for the BLFs distribution and at more backward angles in the case of the TLFs the statistics decrease abruptly. This does not happen as a result of the reaction mechanism. This effect happens since the TLF recoils at high angles have a low velocity. The maximum velocities of the binary partners in this reaction are of the order of $\beta \approx 11\%$. Therefore the prompt γ rays emitted in flight were heavily Doppler shifted. However, it is possible to correct the prompt γ-ray energies for the Doppler effect on an event-by-event basis using the interaction position of the recoils, as measured by Chico. Assuming conservation of linear angular momentum for the scattered beam and target $\cos\theta = \sin\theta_R \sin\theta \cos\varphi_R \cos\varphi + \sin\varphi R \sin\varphi + \cos\theta_R \cos\theta$ where θ_R and φ_R are the scattering angles of the recoils and θ and φ are the detection angles of the γ rays in Gammasphere. The polar angle θ for Gammasphere are listed in Table. The γ-ray energies as measured in the laboratory frame can thus be Doppler corrected for the BLFs or TLFs. Note that in each case only the γ rays emitted by the nuclei for which the Doppler correction is made are enhanced in the resulting spectrum, while those with the incorrect Doppler correction will be smeared out. This technique provides a powerful way of separating the γ rays emitted from the BLFs and TLFs. Figure shows the prompt γ rays which were measured to be within $\Delta t = \pm 45$ns of the master trigger, with no Doppler correction applied.

REFERENCES

C. J. Gallagher and S. A. Moszkowski (1958). Phys. Rev. 111, 1282.

De Shalit and H. Feshbach (1974). Theoretical Nuclear Physics Vol 1: Nuclear Structure, John Wiley and Sons Inc., New York.

E. Der Mateosian and A.W. Sunyar (1974). Atomic Data and Nuclear Data Table 13, 407.

F. Rosel et. al. (1978). Atomic Data and Nuclear Data Table 21, p. 91.

G. F. (1989). Knoll, Radiation Detection and Measurement (Wiley) Singapore.

H. Freiesleben and J. V. Kratz (1984). Phys. Rep. 106, p. 1.

I. Y. Lee et. al. (1997). Phys. Rev. C 56, p. 753.

J. Kantele (1984). Heavy Ions and Nuclear Structure, vol 5, Nuclear Science Research Conferences Series, B. Sikora and Z. Wilhemi, Harwood, 391.

J. M. Blatt and V.F. Wiesskopf (1952). Theoretical Nuclear Physics, John Wiley and Sons Inc., New York (1952).

J.F. Cocks et. al. (1997). Phys. Rev. Lett. 78, p. 2920.

K. Jain et. al. (1994). Phys. Lett. B 322, p. 27.

K. S. Krane (1998). Introductory Nuclear Physics, John Wiley and Sons, New York.

K. Siegbahn (1965). Alpha, Beta, and Gamma-Ray Spectroscopy, North-Holland Publishing Company.

K. Van Bibber et. al. (1977). Phys. Rev. Lett. 38, p. 334.

L. Corradi et. al. (1996). Phys. Rev. C 54, p. 201.

L. Corradi et. al. (1997). Phys. Rev. C 56, p. 938.

L. Corradi et. al. (2000). Phys. Rev. C 61, 024609.

P. Fr¨obrich and R. Lipperheide (1996). Theory of Nuclear Reactions, Oxford, University Press.

R. Albrecht et. al. (1975). Phys. Rev. Lett. 34, p. 1400.

R. Broda et. al., Phys. Rev. Lett. 68, 1671 (1992).

S. J. Asztalos et. al. (1999). Phys. Rev. C 60, 044307.

W. Krolas et. al. (2003). Nucl. Phys. A 724, p. 289.

Corresponding Author

Nidhi Sharma*

M.Sc. Physics, B.Ed., #449, Sector-13, Urban Estate, Kurukshetra, Haryana, India

E-Mail –